EURASIP Journal on Applied Signal Processing 2005:6, 852–860

Turbo-per-Tone Equalization for ADSL Systems

Hilde Vanhaute
ESAT/SCD, Katholieke Universiteit Leuven, Kasteelpark Arenberg 10, 3001 Heverlee, Belgium
Email: hilde.vanhaute@esat.kuleuven.ac.be

Marc Moonen
ESAT/SCD, Katholieke Universiteit Leuven, Kasteelpark Arenberg 10, 3001 Heverlee, Belgium
Email: marc.moonen@esat.kuleuven.ac.be

Received 9 October 2003; Revised 27 August 2004

We study the equalization procedure in discrete multitone (DMT)-based systems, in particular, in DMT-based ADSL systems. Traditionally, equalization is performed in the time domain by means of a channel shortening filter. Shifting the equalization operations to the frequency domain, as is done in per-tone equalization, increases the achieved bitrate by 5–10%. We show that the application of the turbo principle to per-tone equalization can provide significant additional gains. In the proposed receiver structure, referred to as a "turbo-per-tone equalization" structure, equalization and decoding are performed in an iterative fashion. Equalization is done by means of a linear minimum mean squared error (MMSE) equalizer, using a priori information. We give a description of an efficient implementation of such an equalizer in the per-tone structure. Simulations show that we obtain a bitrate increase of 12–16% compared to the original per-tone equalization-based receiver structure.

Keywords and phrases: ADSL, multicarrier modulation, turbo equalization.

1. INTRODUCTION

Discrete multitone (DMT) modulation has become an important transmission method, for instance, for asymmetric digital subscriber line (ADSL), which provides a high bit rate downstream channel and a lower bit rate upstream channel over twisted-pair copper wire. DMT divides the available bandwidth into parallel subchannels or tones, which are quadrature amplitude modulated (QAM) by the incoming bit stream. After modulation with an inverse fast Fourier transform (IFFT), a cyclic prefix is added to each symbol. If the channel impulse response (CIR) order is less than or equal to the cyclic prefix length, demodulation can be implemented by means of an FFT, followed by a (complex) 1-tap frequency-domain equalizer (FEQ) for each tone to compensate for the channel amplitude and phase effects. A long prefix however results in a large overhead with respect to the data rate. An existing solution for this problem, currently used in ADSL, is to insert a (real) T-tap *time-domain equalizer (TEQ)* before demodulation to shorten the channel impulse response. Many algorithms have been developed to initialize the TEQ (e.g., [1, 2, 3]). However a general disadvantage is that the TEQ equalizes all tones simultaneously and as a result limits the performance.

As an alternative to time-domain equalization, *per-tone equalization (PTEQ)* is proposed in [4]. The equalization is now carried out in the frequency domain with a (complex) multitap FEQ for each tone. This receiver scheme always results in a better performance while complexity during transmission is kept at the same level.

In this paper, we apply the *turbo principle* in a per-tone equalization-based receiver to further improve the performance [5]. Turbo techniques have gained a lot of interest since the introduction of the successful turbo codes in 1993 [6]. The underlying iterative receiver scheme, originally developed for parallel concatenated convolutional codes, is now adopted in several other functional blocks, such as trellis-coded modulation (TCM) [7], code-division multiple access (CDMA) [8], turbo equalization [9, 10, 11]. In each of these systems, suboptimal joint detection and decoding is performed through the iterative exchange of soft information between soft-input/soft-output (SISO) components.

This paper is organized as follows. We start with a description of the data model for a per-tone equalization-based DMT system in Section 2. In Section 3, turbo-per-tone equalization is derived. Approximations are considered in Sections 4 and simulation results are given in Section 5.

Notation

Vectors consisting of time-domain samples or elements are written in bold letters and are considered to be column vectors, while frequency-domain scalars and vectors are denoted

by capital letters. Matrices are written in bold capital letters. $\mathbf{0}_{M\times N}$ is the all-zero matrix and $\mathbf{I}_N$ the $N \times N$ identity matrix. $\mathcal{F}_N$ is the $N \times N$ DFT matrix and $\mathcal{I}_N$ is the $N \times N$ IDFT matrix. $(\cdot)^*$ takes the conjugate of the argument, $(\cdot)^{\mathrm{H}}$ is the Hermitian operator and $(\cdot)^{\mathrm{T}}$ the transpose. $\Re\{\cdot\}$ and $\Im\{\cdot\}$ select the real, respectively, imaginary part of a complex argument. $\mathcal{E}\{\cdot\}$ is the expectation operator (where $\mathcal{E}\{x\}$ is often abbreviated to $\bar{x}$) and the covariance operator $\mathrm{Cov}(\mathbf{x}, \mathbf{y})$ is given by $\mathcal{E}\{\mathbf{x}\mathbf{y}^{\mathrm{H}}\} - \mathcal{E}\{\mathbf{x}\}\mathcal{E}\{\mathbf{y}^{\mathrm{H}}\}$.

2. DATA MODEL FOR A PER-TONE EQUALIZATION-BASED DMT RECEIVER

The following notation is adopted in the description of the DMT system. N is the symbol size expressed in number of samples and k is the time index of a symbol $X_n^{(k)}$ for tone n ($n = 1, \ldots, N$) to be transmitted at symbol period k. $X_n^{(k)}$ is taken from the 2^{Q_n}-ary QAM constellation $\mathcal{S}_n = \{\alpha_1, \alpha_2 \cdots \alpha_{M_n}\}$ ($M_n = 2^{Q_n}$) with Q_n the number of bits on tone n, and vector $X_{1:N}^{(k)}$ denotes $[X_1^{(k)} \cdots X_N^{(k)}]^{\mathrm{T}}$. $Y_n^{(k)}$ is the demodulated output for tone n (after the FFT) and $\hat{X}_n^{(k)}$ the symbol estimate (after per-tone equalization). Note that $X_{N-(n-2)}^{(k)} = (X_n^{(k)})^*$, $n = 2, \ldots, (N/2)$, and that similar equations hold for $Y_n^{(k)}$. The index $N - (n-2)$ will be denoted as n^*. Further, ν is the length of the cyclic prefix and $s = N + \nu$ the length of a symbol including prefix. Finally, n_l is additive channel noise and y_l is the received (time-domain) signal with l the sample index.

To describe the data model, we consider three successive symbols $X_{1:N}^{(t)}$ to be transmitted at $t = k-1, k, k+1$, respectively. The kth symbol is the symbol of interest, the previous and the next symbol are used to include interferences from neighboring symbols in our model. T is the equalizer length. The received signal may then be specified as follows:

$$\begin{bmatrix} y_{ks+\nu-T+2} \\ \vdots \\ y_{(k+1)\cdot s} \end{bmatrix} = \mathbf{H} \begin{bmatrix} X_{1:N}^{(k-1)} \\ X_{1:N}^{(k)} \\ X_{1:N}^{(k+1)} \end{bmatrix} + \begin{bmatrix} n_{ks+\nu-T+2} \\ \vdots \\ n_{(k+1)\cdot s} \end{bmatrix} \quad \text{or} \quad \mathbf{y} = \mathbf{H}\mathbf{X} + \mathbf{n}, \tag{1}$$

where $\mathbf{H}_{(N+T-1)\times 3N}$ includes modulation with IFFT, adding of prefix and channel convolution. The channel impulse response is assumed to be known at the receiver.

At the receiver, per-tone equalization (PTEQ) is performed as described in [4]. The PTEQ coefficients can be viewed as a complex multitap FEQ per-tone. For each tone n, the equalizer input $\mathbf{z}_n$ consists of $T-1$ (real) difference terms $\Delta\mathbf{y} = [y_{ks+\nu-(T-2)} - y_{(k+1)s-(T-2)} \quad \cdots \quad y_{ks+\nu} - y_{(k+1)s}]^{\mathrm{T}}$, and the nth output $Y_n^{(k)}$ of the FFT:

$$\mathbf{z}_n = \begin{bmatrix} \Delta\mathbf{y} \\ Y_n^{(k)} \end{bmatrix} = \underbrace{\left[\begin{array}{c|c|c} \mathbf{I}_{T-1} & \mathbf{0} & -\mathbf{I}_{T-1} \\ \hline \mathbf{0} & \mathcal{F}_N(n,:) & \end{array}\right]}_{\mathbf{F}_n} \cdot \mathbf{y}, \tag{2}$$

with $\mathbf{F}_n$ a $T \times (N + T - 1)$ matrix (a modified sliding FFT, see [4]). We can rewrite this input $\mathbf{z}_n$ as

$$\begin{aligned} \mathbf{z}_n &= \mathbf{F}_n(\mathbf{H}\mathbf{X} + \mathbf{n}) \\ &= \mathbf{G}_n\mathbf{X} + \mathbf{N}_n, \end{aligned} \tag{3}$$

with $\mathbf{G}_n$ a $(T \times 3N)$ matrix and $\mathbf{N}_n$ a noise vector of length T. The equalizer output, that is, the estimate $\hat{X}_n^{(k)}$ of the transmitted symbol $X_n^{(k)}$, is obtained as

$$\hat{X}_n^{(k)} = \mathbf{v}_n^{\mathrm{H}} \cdot \mathbf{z}_n \tag{4}$$

with $\mathbf{v}_n$ the T-tap per-tone equalizer for tone n. These equalizer coefficients can then be optimized by solving a least-square problem for each tone separately, hence the term "per-tone equalization." In general, giving each tone its optimal equalizer leads to a 5–10% performance improvement over time-domain equalization-based demodulation. For more details, the reader is referred to [4].

3. TURBO-PER-TONE EQUALIZATION

3.1. General description

In a turbo equalization system, suboptimal joint equalization and decoding is performed through the iterative exchange of soft information between a soft-input/soft-output (SISO) equalizer and a SISO decoder. This soft information about the transmitted bits $c_{n,j}$ is given as log-likelihood ratios (LLR), defined as follows:

$$L(c_{n,j}) = \log \frac{P(c_{n,j} = 1)}{P(c_{n,j} = 0)}. \tag{5}$$

This information exchange is difficult to realize in a time-domain equalization- (TEQ-) based DMT receiver. Since the output signal of the TEQ is a time-domain signal which does not have a finite alphabet, it is not possible to express LLRs based on these outputs. On the other hand, in a per-tone equalization-based receiver, the equalization is carried out in the frequency domain based on (distorted) QAM symbols. A symbol mapping expresses the relation between the QAM symbols and the coded bits, so LLRs can be easily deduced. Per-tone equalization is thus more suited for the introduction of turbo techniques in the equalization procedure.

A DMT system using turbo-per-tone SISO equalization and SISO decoding at the receiver is depicted in Figure 1. A fundamental property of a SISO component is that the calculated a posteriori LLR L_p can always be split up into an a priori term L_a and *extrinsic* information L_e:

$$L_p(c_{n,j}) = L_e(c_{n,j}) + L_a(c_{n,j}). \tag{6}$$

The extrinsic LLR can be viewed as an update of the available a priori information on the bit c_n, obtained through equalization or decoding. This extrinsic information, delivered by one component, is used as a priori information by the other component, after (de-)interleaving, as can be seen in Figure 1.

The SISO decoder uses the optimal (log-)MAP (maximum a posteriori) algorithm, or a suboptimal version of it (max-log-MAP or SOVA) [12]. The SISO equalizer, as it was first proposed by Douillard et al. [9], also applies the MAP algorithm to the underlying trellis of the channel convolution. However, for long channel impulse responses and/or large symbol alphabets, this MAP-based equalization suffers from impractically high computational complexity. A suboptimal,

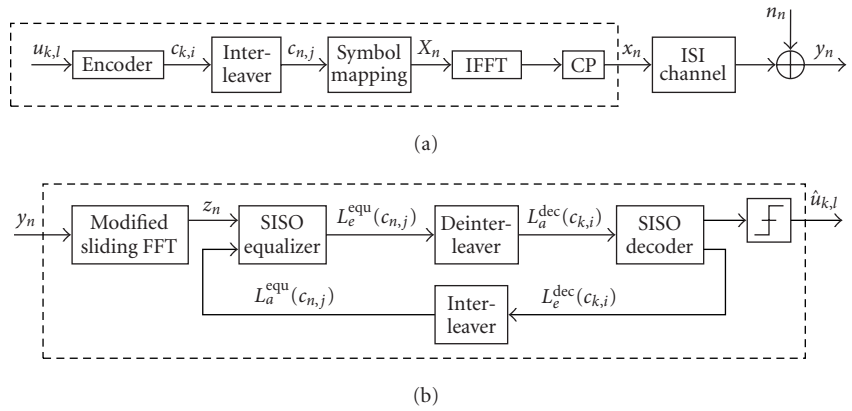

Figure 1: A turbo-per-tone equalization-based DMT system: (a) DMT transmitter; (b) DMT receiver based on a turbo-per-tone equalizer.

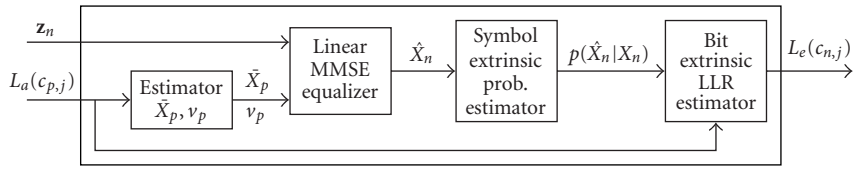

Figure 2: SISO equalizer based on MMSE equalization.

reduced-complexity solution is to replace the MAP equalizer by linear processing of the received signal, in the presence of a priori information about the transmitted data. Several algorithms can be found, such as linear equalization based on the minimum mean squared error (MMSE) criterion [13], soft intersymbol interference (ISI) cancellation [10], or MMSE decision feedback equalization [11]. In this paper, we focus on linear MMSE equalization using a priori information.

3.2. Linear MMSE equalization using a priori information in a per-tone-based receiver

In an SISO equalizer based on MMSE equalization, as illustrated in Figure 2, the mean $\mathcal{E}\{X_p^{(t)}\} \triangleq \bar{X}_p^{(t)}$ and variance $\text{Cov}(X_p^{(t)}, X_p^{(t)}) \triangleq \nu_p^{(t)}$ of the transmitted data symbol $X_p^{(t)}$ are first calculated ($p = 1, \ldots, N$) [13], given the a priori information $L_a^{(t)}(c_{p,j})$, $j = 1, \ldots, Q_p$, with Q_p the number of bits on tone p for DMT symbols $t = k-1, k$, and $k+1$. Then the equalizer estimates $\hat{X}_n^{(k)}$ using the observation $\mathbf{z}_n$ (see (4) and (3)) and taking into account that $\bar{X}_{n^*}^{(k)} = (\bar{X}_n^{(k)})^*$ and $\nu_{n^*}^{(k)} = \nu_n^{(k)}$,

$$\begin{aligned} \hat{X}_n^{(k)} &= \mathbf{w}_n^{\text{H}} \left(\mathbf{z}_n - \mathbf{G}_n \mathcal{E}\{\mathbf{X}\} + \mathbf{g}_n \bar{X}_n^{(k)} + \mathbf{g}_{n^*} \bar{X}_{n^*}^{(k)} \right), \\ \mathbf{w}_n &= \text{Cov}\,(\mathbf{z}_n, \mathbf{z}_n)^{-1}\, \text{Cov}\left(\mathbf{z}_n, X_n^{(k)}\right), \end{aligned} \tag{7}$$

where $\mathbf{g}_n$ is the $(N+n)$th column of $\mathbf{G}_n$. $\mathbf{w}_n$ can be calculated as [13]

$$\begin{aligned} \mathbf{w}_n = \Big[\mathbf{G}_n \mathbf{R}_{\mathbf{XX}} \mathbf{G}_n^{\text{H}} + \left(1 - \nu_n^{(k)}\right) \left(\mathbf{g}_n \mathbf{g}_n^{\text{H}} + \mathbf{g}_{n^*} \mathbf{g}_{n^*}^{\text{H}} \right) \\ + \mathcal{E}\left\{ N_n N_n^{\text{H}} \right\} \Big]^{-1} \mathbf{g}_n, \end{aligned} \tag{8}$$

with $\mathbf{R}_{\mathbf{XX}} = \text{Cov}(\mathbf{X}, \mathbf{X})$. From the independence of the bits $c_{p,j}^{(t)}$, it follows that the symbols $X_p^{(t)}$ are independent and that the covariance matrix $\mathbf{R}_{\mathbf{XX}}$ is a $3N \times 3N$ diagonal matrix with variances $\nu_p^{(t)} = \text{Cov}(X_p^{(t)}, X_p^{(t)})$ on its diagonal ($t = k-1, k, k+1$; $p = 1, \ldots, N$). Further

$$\begin{aligned} \mathcal{E}\left\{ N_n N_n^{\text{H}} \right\} &= \mathbf{F}_n \mathcal{E}\{\mathbf{n}\mathbf{n}^{\text{H}}\} \mathbf{F}_n^{\text{H}} \\ &= \sigma_N^2 \left[\begin{array}{c|c} 2\mathbf{I}_{T-1} & -\mathbf{f}_n \\ \hline -\mathbf{f}_n^{\text{H}} & 1 \end{array} \right], \end{aligned} \tag{9}$$

with $\mathbf{f}_n = \mathcal{F}_N^{\text{H}}(n, N-T+2 : N)$.

After MMSE equalization, we assume that the pdfs $p(\hat{X}_n^{(k)} | X_n^{(k)} = \alpha_i)$, $\alpha_i \in \mathcal{S}_n$, are Gaussian so the parameters $\mu_{n,i}^{(k)} \triangleq \mathcal{E}\{\hat{X}_n^{(k)} | X_n^{(k)} = \alpha_i\}$ and $(\nu_{n,i}^{(k)})^2 \triangleq \text{Cov}(\hat{X}_n^{(k)}, \hat{X}_n^{(k)} | X_n^{(k)} = \alpha_i)$ can be easily calculated [8]. Then these values are used in the estimation of the bit LLRs [8].

3.3. Complexity reduction

For the computation of the equalizer coefficients on tone n, the covariance matrix $\text{Cov}(\mathbf{z}_n, \mathbf{z}_n)$ has to be inverted, see (7). This leads to a high computational complexity, which, however, can be drastically reduced if we exploit the specific PTEQ structure. As can be seen by combining (2) and (3), the first $T-1$ rows of $\mathbf{G}_n$ are common for every tone. We will denote the first $T-1$ rows with the subscript "diff," since they act on or refer to the difference terms.

The covariance matrix can be split into submatrices, corresponding to the structure of $\mathbf{G_n}$ and $\mathcal{E}\{\mathbf{N}_n \mathbf{N}_n^{\text{H}}\}$:

$$\text{Cov}\,(\mathbf{z}_n, \mathbf{z}_n) = \left[\begin{array}{c|c} \mathbf{D}_n & \mathbf{d}_n \\ \hline \mathbf{d}_n^{\text{H}} & u_n \end{array} \right], \tag{10}$$

Table 1: Complexity of the equalization procedure.

Operation		Per iteration
For all tones		
Interference estimation	$\mathbf{G}_{\text{diff}}\mathcal{E}\{\mathbf{X}\}$	$\mathcal{O}(N_u T)$
Equalizer coefficients	$\mathbf{D}$	$\mathcal{O}(N_u T^2)$
	$\mathbf{D}^{-1}$	$\mathcal{O}(T^3)$
Per-tone		
Interference estimation	$2\Re\{\mathbf{g}_{\text{diff},n}\bar{X}_n^{(k)}\}$	$\mathcal{O}(T)$
	$\mathbf{G}_{\text{fft},n}\mathcal{E}\{\mathbf{X}\}$	$\mathcal{O}(N_u)$
Equalizer coefficients	u_n	$\mathcal{O}(N_u)$
	$\mathbf{d}_n$	$\mathcal{O}(N_u T)$
	$\mathbf{D}_n^{-1}$, $[\text{Cov}(\mathbf{z}_n,\mathbf{z}_n)]^{-1}$	$\mathcal{O}(T^2)$
Total (per DMT symbol)		$\mathcal{O}(N_u T(N_u+T))$

where

$$\begin{aligned}\mathbf{D}_n &= \mathbf{D} + \left(1-\nu_n^{(k)}\right)\left(\mathbf{g}_{\text{diff},n}\mathbf{g}_{\text{diff},n}^{\text{H}} + \mathbf{g}_{\text{diff},n^*}\mathbf{g}_{\text{diff},n^*}^{\text{H}}\right)\\ &= \mathbf{D} + 2\left(1-\nu_n^{(k)}\right)\Re\left\{\mathbf{g}_{\text{diff},n}\mathbf{g}_{\text{diff},n}^{\text{H}}\right\}\end{aligned} \tag{11}$$

with

$$\begin{aligned}\mathbf{D} &= \text{Cov}\left(\mathbf{z}_{\text{diff}},\mathbf{z}_{\text{diff}}\right)\\ &= \mathbf{G}_{\text{diff}}\mathbf{R}_{\mathbf{XX}}\mathbf{G}_{\text{diff}}^{\text{H}} + 2\sigma_N^2\mathbf{I}_{T-1}.\end{aligned} \tag{12}$$

$\mathbf{D}$ is a (real) symmetric tone-independent matrix and $\mathbf{D}_n$ is a rank-1 modification of $\mathbf{D}$ to eliminate a priori information of tones n and n^*. $\mathbf{G}_{\text{diff}}$ is a $(T-1)\times 3N$ matrix. The 3rd equality follows from the fact that $\mathbf{g}_{\text{diff},n^*} = \mathbf{g}_{\text{diff},n}^*$. The inverse of the covariance matrix can also be split into submatrices:

$$\left[\text{Cov}\left(\mathbf{z}_n,\mathbf{z}_n\right)\right]^{-1} = \left[\begin{array}{c|c}\mathbf{B}_n & \mathbf{b}_n\\ \hline \mathbf{b}_n^{\text{H}} & t_n\end{array}\right]. \tag{13}$$

By expressing that the product $\text{Cov}(\mathbf{z}_n,\mathbf{z}_n)\times[\text{Cov}(\mathbf{z}_n,\mathbf{z}_n)]^{-1}$ should be equal to the identity matrix, the submatrices $\mathbf{B}_n$, $\mathbf{b}_n$ and t_n can be found as follows:

$$\begin{aligned}\mathbf{p}_n &= \mathbf{D}_n^{-1}\mathbf{d}_n,\\ t_n &= \frac{1}{u_n - \mathbf{d}_n^{\text{H}}\mathbf{p}_n},\\ \mathbf{b}_n &= -\mathbf{p}_n t_n,\\ \mathbf{B}_n &= \mathbf{D}_n^{-1} - \mathbf{b}_n\mathbf{p}_n^{\text{H}}.\end{aligned} \tag{14}$$

In this computation, $\mathbf{D}_n^{-1}$ is needed. This inverse can be calculated in an efficient way. Therefore, write $\mathbf{D}_n$ as

$$\mathbf{D}_n = \mathbf{D} + \mathbf{a}\mathbf{a}^{\text{H}} + \left(\mathbf{a}\mathbf{a}^{\text{H}}\right)^{\text{T}} \tag{15}$$

with $\mathbf{a} = \sqrt{1-\nu_n}\cdot\mathbf{g}_{\text{diff},n}$, and define

$$\begin{aligned}\mathbf{q}_n &= \mathbf{D}^{-1}\mathbf{a}_n,\\ c_n &= \mathbf{a}_n^{\text{T}}\mathbf{q}_n = \mathbf{q}_n^{\text{T}}\mathbf{a}_n \in \mathbb{C},\\ d_n &= \mathbf{a}_n^{\text{H}}\mathbf{q}_n = \mathbf{q}_n^{\text{H}}\mathbf{a}_n \in \mathbb{R}.\end{aligned} \tag{16}$$

By applying the matrix inversion lemma[1] twice, it can be shown that this inverse is equal to

$$\mathbf{D}_n^{-1} = \mathbf{D}^{-1} - \frac{2(1+d_n)\Re\left\{\mathbf{q}_n\mathbf{q}_n^{\text{H}}\right\} - 2\Re\left\{c_n^*\mathbf{q}_n\mathbf{q}_n^{\text{T}}\right\}}{(1+d_n)^2 - |c_n|^2}. \tag{17}$$

The $\mathbf{D}^{-1}$ obviously should be calculated only once. This reduces the complexity of inverting $\mathbf{D}_n$ for all tones together from $\mathcal{O}(N_u T^3)$ to $\mathcal{O}(T^3 + N_u T^2)$, with N_u the number of used tones. The complexity of the equalization procedure is summarized in Table 1. Typical values for downstream transmission are $N_u \approx N_{\text{FFT}}/2 = 256$ and $T = 16$, leading to a total complexity of $\mathcal{O}(N_u T(N_u+T))$ (per iteration).

4. APPROXIMATE IMPLEMENTATION

The equalizer filter coefficients have to be updated for every tone and for every iteration, based on the available a priori information. To reduce this computational burden, we introduce some approximations.

(i) *Fixed equalizer coefficients in the first iteration*. We can assume that the *previous symbol* $X_{1:N}^{(k-1)}$ is perfectly known from the previous equalization and decoding step, which gives a zero variance for all the tones of the previous symbol. Moreover, there is no a priori information available about the *symbol of interest* $X_{1:N}^{(k)}$ nor about the *next symbol* $X_{1:N}^{(k+1)}$. This leads to fixed equalizer coefficients for the first iteration which can be initialized before transmission. Only the mean of the previous symbol has to be computed. The initialization complexity is given in Table 1. In this way, the equalization in the first iteration is similar to the conventional per-tone equalization, with the only difference that the estimation of the interference of the previous symbol is subtracted.

(ii) *Partial iterative equalizer*. Although the majority of the intersymbol and intercarrier interference (ISI and ICI) is already removed after the first iteration, the matched-filter (MF) bound is not completely reached, especially on the lowest tones located near the cutoff frequencies of the front-end filters, see Figure 3. These tones are impaired by more

[1] More specifically, if $\mathbf{A} = \mathbf{B} + \mathbf{c}\mathbf{c}^{\text{H}}$, then $\mathbf{A}^{-1} = \mathbf{B}^{-1} - \mathbf{B}^{-1}\mathbf{c}\mathbf{c}^{\text{H}}\mathbf{B}^{-1}/(1+\mathbf{c}^{\text{H}}\mathbf{B}^{-1}\mathbf{c})$.

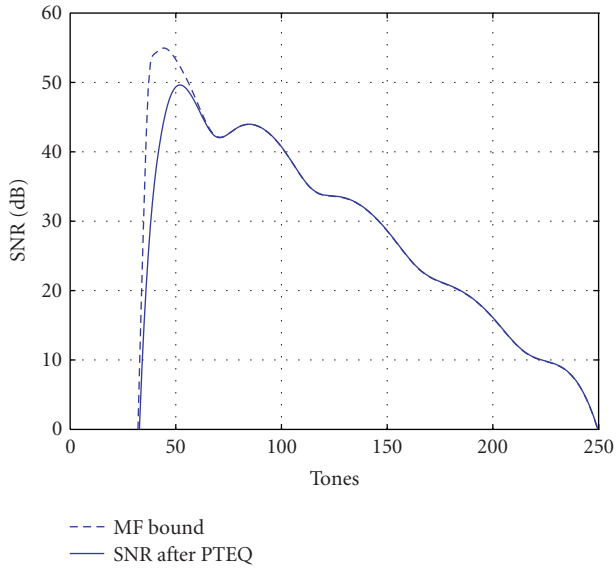

Figure 3: Matched-filter bound and SNR obtained after the first iteration for a downstream ADSL channel (number of taps $T = 16$).

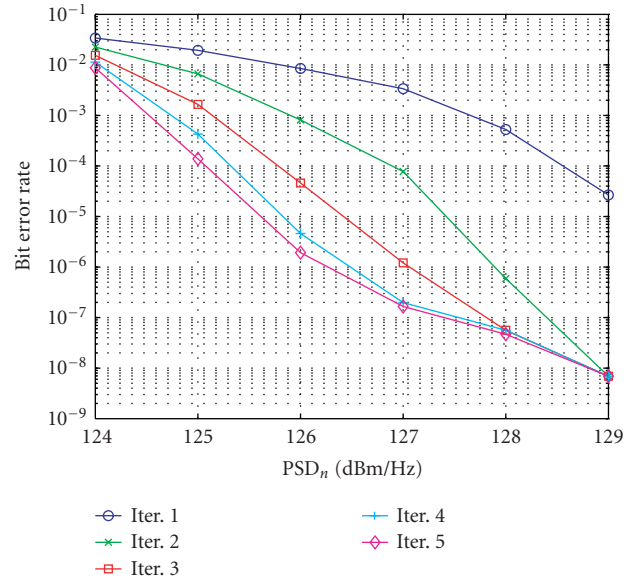

Figure 4: BER versus PSD of the noise in the turbo-per-tone equalization-based scheme.

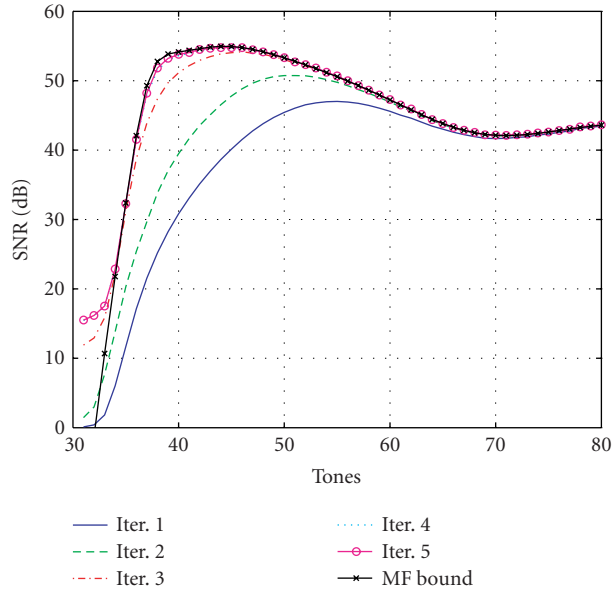

Figure 5: SNR improvement in the turbo-per-tone equalization-based scheme with $T = 8$ and PSD$_n = -127$ dBm/Hz.

interference due to the nonlinear phase properties of these filters. Since most of the tones already almost have maximum SNR, there is no need to reestimate these tones by means of iterative equalization. Only the lowest tones, for instance, up to tone 80, are iteratively equalized. This partial iterative equalization results in a complexity $\mathcal{O}(N_u T(T + N_{u,2}))$ with $N_{u,2}$ the number of used tones which are reestimated from the second iteration. For the given channel and background noise, $N_{u,2} \approx N_u/4$. However, the bit extrinsic LLRs still have to be computed for each tone and in every iteration, based on the estimate of the transmitted symbol $\hat{X}_n^{(k)}$ and the available a priori information (see Figure 2).

Simulations have shown that the number of equalizer taps can be reduced compared to the noniterative per-tone equalizer-based receiver. However, the fewer taps are used, the more iterations are needed to obtain the same bit error rate.

5. SIMULATION RESULTS

Time-domain simulations were performed for an ANSI downstream ADSL loop (ANSI13 [14]) with additive white Gaussian noise. The power spectral density (PSD) of the transmitted signal was -40 dBm/Hz while the PSD of the noise was varied between -124 and -129 dBm/Hz. For the encoding, we chose a rate $R = 9/10$ recursive systematic convolutional (RSC) code of order 4, with an octal representation [15 31 37 27 25 13 21 23 33 35], as described in [15]. The interleaver length is 1780, being the total number of bits included in one DMT symbol.

Natural mapping was selected for square constellations, since natural mapping has a better performance than Gray mapping in iterative schemes [16]. The number of equalization taps was set to $T = 8$. The MAP decoding is done using the dual code as described in [17]. Since the trellis is not terminated, the last bits of the decoded sequence are more sensitive to errors. If we force the (de)interleaver to map well-conditioned bits onto the end of the coded sequence, we can reduce the BER at the end of the codeword.

From the second iteration, only the tones between tone 31(= lowest used tone)[2] and tone 80 are reestimated (i.e., 50 tones out of a total number of 213 used tones). The number of iterations was set to 5. Figure 4 shows the bit error rate (BER) versus the PSD of the noise (PSD$_n$). In Figure 5, it is depicted how the SNR on the lowest used tones

[2]Tones 31 to 37 can be used in an echo-cancelled system.

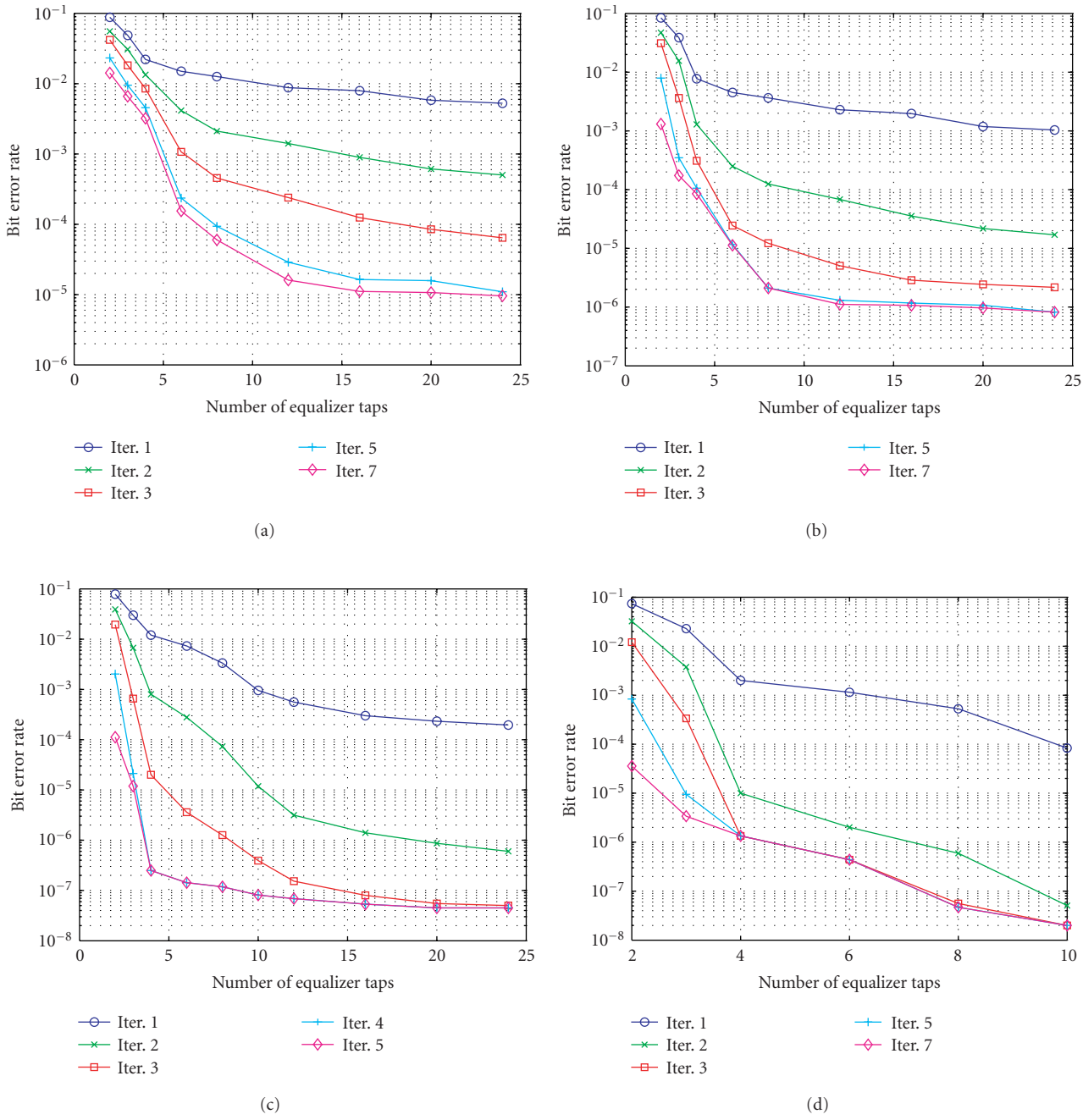

FIGURE 6: BER versus number of taps in the turbo-per-tone equalization-based scheme for different noise PSDs: (a) $\mathrm{PSD}_n = -125$ dBm/Hz, (b) $\mathrm{PSD}_n = -126$ dBm/Hz, (c) $\mathrm{PSD}_n = -127$ dBm/Hz, and (d) $\mathrm{PSD}_n = -128$ dBm/Hz.

improves throughout iterations (for a PSD of the noise of −127 dBm/Hz). After 5 iterations, the SNR after the MMSE equalization actually reaches the matched-filter bound.

Next, we varied the noise and the numbers of equalization taps. Figure 6 shows the BER performance for the different numbers of taps and different noise PSDs (−125 to −128 dBm/Hz). When less taps are used, almost the same BER can be achieved but more iterations are needed. Vice versa, less iterations are needed when more taps are used. It can also be noted that for higher SNR, less iterations are needed to reach convergence.

The comparison between the original per-tone equalization and the turbo-per-tone equalization is based on equal target bit error rates (BERs) for both schemes. The performance is then measured by the achievable capacity (bps). The turbo scheme is initialized with a certain bit loading, which gives rise to a specific BER for every iteration, whereas in the original per-tone scheme, the bit loading is calculated given

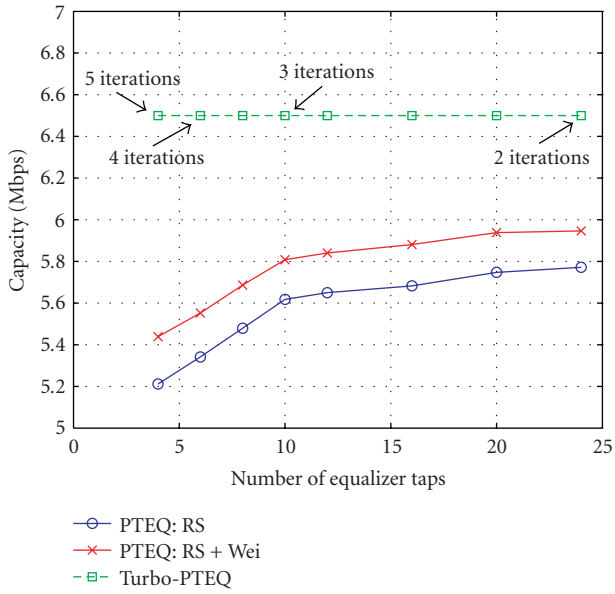

Figure 7: Capacity versus number of equalizer taps.

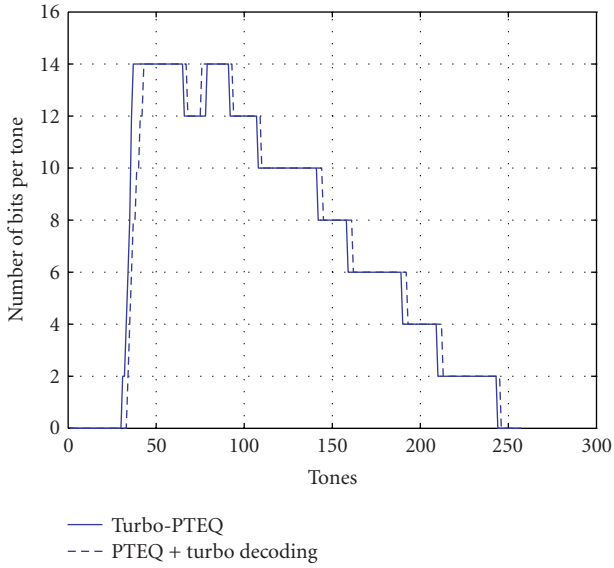

Figure 8: Bit loading for the turbo-PTEQ-based scheme ($T = 8$) and for conventional PTEQ ($T = 16$) followed by a turbo decoder. The total number of bits per DMT symbol is 1780 bits for both schemes.

the BER. For noninteger bit loading, we have[3]

$$b = \sum_n b_n = \sum_n \log_2\left(1 + \frac{\mathrm{SNR}_n \cdot \gamma_c}{\Gamma}\right), \tag{18}$$

with γ_c the coding gain and Γ the SNR gap, which expresses the distance between the theoretical Shannon capacity and the practically achievable bit rate. The ADSL standard provides Reed-Solomon (RS) codes for the error correction with a coding gain of 3 dB. The standard states that as an option a 4D 16-state trellis code (the Wei code) can be concatenated with an RS code. This concatenated coding scheme results in a coding gain of 5.2 dB.

The SNR gap depends on the target BER, which is set to $5 \cdot 10^{-7}$. For a noise PSD of -127 dBm/Hz, one can see from Figure 6c that this BER can be reached in the turbo scheme with 5 iterations when 4 taps are used, with 4 iterations when 6 taps are used, with 3 iterations when 10 taps are used, or with 2 iterations when 24 taps are used. The capacity of the turbo-PTEQ follows from the bit loading and results in 6.50 Mbps. This is compared to the original PTEQ with two different coding schemes and different number of equalizer taps in Figure 7. It can be seen that the turbo-PTEQ performs 12 to 16% better than the PTEQ scheme with 10 taps and 9 to 13% better than the PTEQ scheme with 24 taps.

The turbo-PTEQ-based scheme is also compared with a system that consists of a cascade of a conventional PTEQ and a turbo decoder. The encoder consists of 2 parallel concatenated RSC codes of order 4 with a code rate of 18/19. In this way, the concatenated scheme has the same code rate as in the turbo-per-tone equalization scheme: 18 information bits are encoded into 18 systematic bits and 2 parity bits, one from each constituent encoder. Decoding is performed using the dual code. The DMT block size is also set to 1780 bits, but with a slightly different bit loading, depending on the number of equalizer taps used, since the lowest tones cannot carry as much bits as in the turbo-PTEQ scheme. Two different bit loadings are given in Figure 8. The obtained BERs are shown in Figure 9 for different number of taps in the turbo-coded system and for different noise PSDs (-125 tot -128 dBm/Hz). When only a small number of taps are used, there is almost no improvement performing iterations. In general, convergence is reached after 2 iterations. Comparing the turbo-per-tone equalization and the turbo-coded scheme, it can be seen that, for the same number of taps, the turbo-coded system has a better performance in the first and the second iteration, but in further iterations the turbo-per-tone equalizer outperforms the turbo-coded system, especially for high SNRs and for a moderate number of taps ($T < 20$). If we now set the target BER to $5 \cdot 10^{-7}$, we can deduce from Figures 6 and 9 how many iterations are required to obtain this BER for a certain number of taps. This is depicted in Figure 10. In the turbo-coded scheme at least 12 taps are needed with a noise PSD of -127 dBm/Hz to reach this BER, whereas in the turbo-PTEQ-based scheme, for instance, 6 taps are sufficient, but one more iteration is required.

6. CONCLUSIONS

In this paper, we have introduced the turbo principle in per-tone equalization for DMT-ADSL modems. A receiver scheme, where equalization and decoding are performed in an iterative fashion, was presented. We have proposed to perform iterative equalization only on the tones where SNR improvement is still possible. It is shown that with the turbo-per-tone scheme the matched-filter bound can be well approximated on all tones, and that this scheme performs

[3]There is no noise margin included in this calculation.

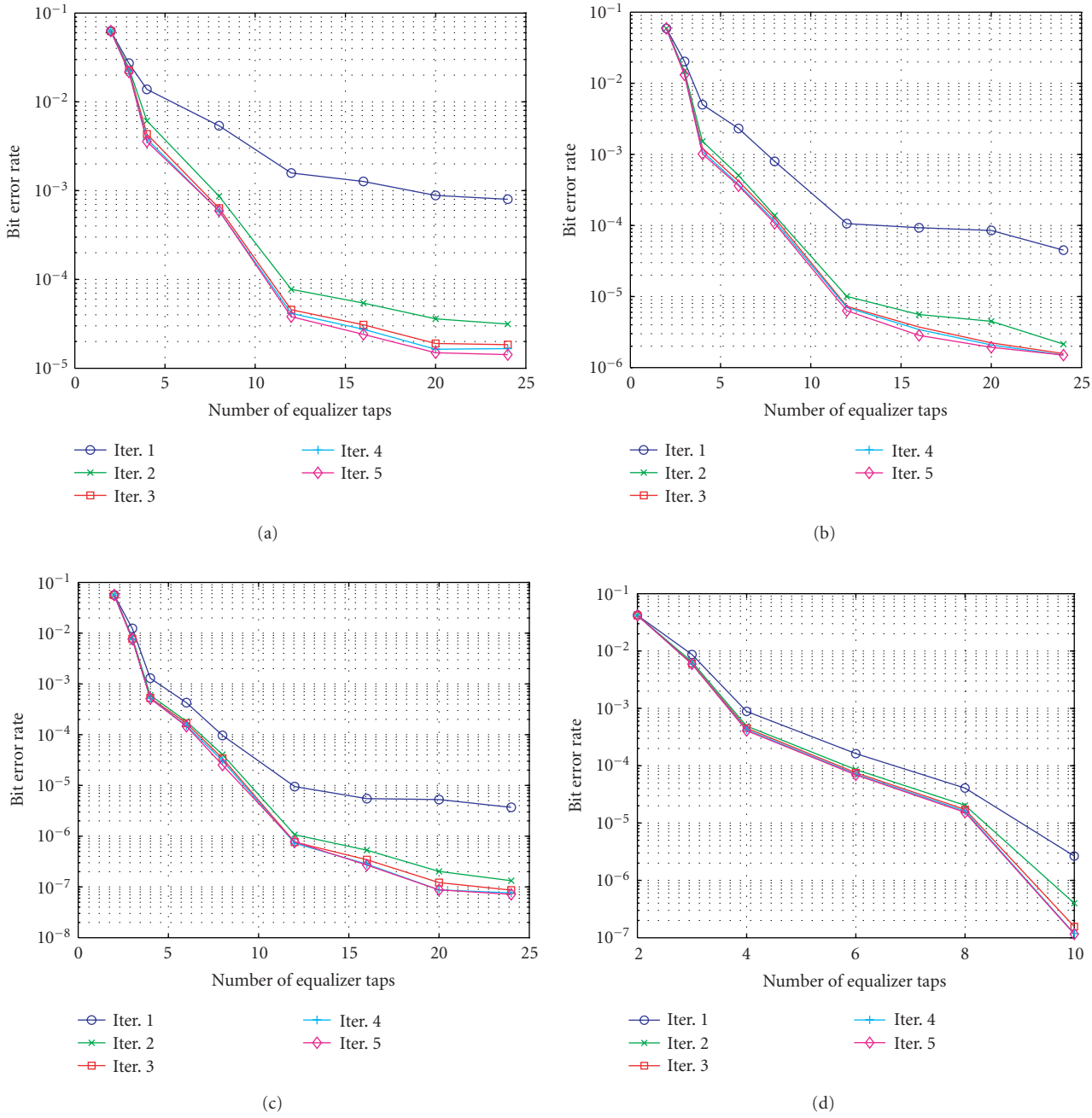

FIGURE 9: BER versus number of taps in the turbo-coded scheme for different noise PSDs: (a) $\mathrm{PSD}_n = -125$ dBm/Hz, (b) $\mathrm{PSD}_n = -126$ dBm/Hz, (c) $\mathrm{PSD}_n = -127$ dBm/Hz, (d) $\mathrm{PSD}_n = -128$ dBm/Hz.

significantly better than the original per-tone scheme. We have also shown that the turbo-per-tone equalizer outperforms a concatenated system consisting of a per-tone equalizer and turbo decoding. Utilizing a turbo code instead of a convolutional code in the proposed turbo-per-tone equalization would increase the performance even further, but results in a higher computational complexity. This setup is therefore not considered in this paper since further reduction of the complexity is still necessary and will be the subject of further research.

ACKNOWLEDGMENTS

This research work was carried out at the ESAT Laboratory of the Katholieke Universiteit Leuven, in the frame of the Belgian Programme on Interuniversity Attraction Poles, initiated by the Belgian Federal Science Policy Office IUAP P5/22 and P5/11, the Concerted Research Action GOA-MEFISTO-666, Research Project FWO no. G.0196.02, and the IWT Project 030054: SOLIDT. The scientific responsibility is assumed by its authors.

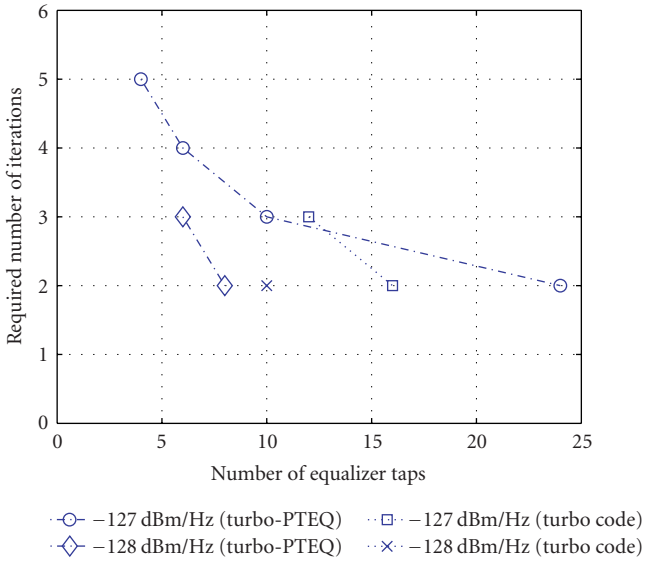

FIGURE 10: Required number of iterations to obtain a target BER of $5 \cdot 10^{-7}$ for the turbo-PTEQ scheme and the turbo-coded scheme.

REFERENCES

[1] N. Al-Dhahir and J. M. Cioffi, "Optimum finite-length equalization for multicarrier transceivers," *IEEE Trans. Commun.*, vol. 44, no. 1, pp. 56–64, 1996.

[2] B. Farhang-Boroujeny and M. Ding, "Design methods for time-domain equalizers in DMT transceivers," *IEEE Trans. Commun.*, vol. 49, no. 3, pp. 554–562, 2001.

[3] G. Arslan, B. L. Evans, and S. Kiaei, "Equalization for discrete multitone transceivers to maximize bit rate," *IEEE Trans. Signal Processing*, vol. 49, no. 12, pp. 3123–3135, 2001.

[4] K. Van Acker, G. Leus, M. Moonen, O. van de Wiel, and T. Pollet, "Per tone equalization for DMT-based systems," *IEEE Trans. Commun.*, vol. 49, no. 1, pp. 109–119, 2001.

[5] H. Vanhaute and M. Moonen, "Turbo per tone equalization for ADSL systems," in *Proc. IEEE International Conference Communications (ICC '04)*, vol. 1, pp. 6–10, Paris, France, June 2004.

[6] C. Berrou, A. Glavieux, and P. Thitimajshima, "Near Shannon limit error-correcting coding and decoding: turbo codes," in *Proc. IEEE International Conference on Communications (ICC '93)*, vol. 2, pp. 1064–1070, Geneva, Switzerland, May 1993.

[7] S. Benedetto, D. Divsalar, G. Montorsi, and F. Pollara, "Parallel concatenated trellis coded modulation," in *Proc. IEEE International Conference on Communications (ICC '96)*, vol. 2, pp. 974–978, Dallas, Tex, USA, June 1996.

[8] X. Wang and H. V. Poor, "Iterative (turbo) soft interference cancellation and decoding for coded CDMA," *IEEE Trans. Commun.*, vol. 47, no. 7, pp. 1046–1061, 1999.

[9] C. Douillard, M. Jézéquel, C. Berrou, A. Picart, P. Didier, and A. Glavieux, "Iterative correction of intersymbol interference: turbo-equalization," *European Transactions on Telecommunication*, vol. 6, no. 5, pp. 507–511, 1995.

[10] A. Glavieux, C. Laot, and J. Labat, "Turbo equalization over a frequency selective channel," in *Proc. International Symposium Turbo Codes & Related Topics*, pp. 96–102, Brest, France, September 1997.

[11] M. Tüchler, R. Koetter, and A. C. Singer, "Turbo equalization: principles and new results," *IEEE Trans. Commun.*, vol. 50, no. 5, pp. 754–767, 2002.

[12] P. Robertson, E. Villebrun, and P. Höher, "A comparison of optimal and sub-optimal MAP decoding algorithms operating in the log domain," in *Proc. IEEE International Conference Communications (ICC '95)*, vol. 2, pp. 1009–1013, Seattle, Wash, USA, June 1995.

[13] M. Tüchler, A. C. Singer, and R. Koetter, "Minimum mean squared error equalization using a priori information," *IEEE Trans. Signal Processing*, vol. 50, no. 3, pp. 673–683, 2002.

[14] K. Sistanizadeh, "Proposed canonical loops for ADSL and their loss characteristics," Tech. Rep. 91-116, ANSI T1E1.4 Committee Contribution, August 1991.

[15] A. Graell i Amat, S. Benedetto, and G. Montorsi, "High-rate convolutional codes: search, efficient decoding and applications," in *Proc. Information Theory Workshop*, pp. 37–40, Bangalore, India, October 2002.

[16] S. ten Brink, J. Speidel, and R.-H. Yan, "Iterative demapping and decoding for multilevel modulation," in *Proc. IEEE Global Telecommunications Conference (Globecom '98)*, vol. 1, pp. 579–584, Sydney, Australia, November 1998.

[17] S. Riedel, "MAP decoding of convolutional codes using reciprocal dual codes," *IEEE Trans. Inform. Theory*, vol. 44, no. 3, pp. 1176–1187, 1998.

Hilde Vanhaute was born in Menen, Belgium, in 1978. In 2001, she received the M.S. degree in electrical engineering from the Katholieke Universiteit Leuven (K. U. Leuven), Leuven, Belgium. Currently, she is pursuing the Ph.D. degree as a Research Assistant at the SCD Laboratory, the Department of Electrical Engineering (ESAT), Katholieke Universiteit Leuven, Leuven, Belgium. From 2002 till now, she is supported by the Flemish Institute for Scientific and Technological Research in Industry (IWT). Her research interests are in the area of digital signal processing for DSL communications under the supervision of Marc Moonen.

Marc Moonen received the Electrical Engineering degree and the Ph.D. degree in applied sciences from the Katholieke Universiteit Leuven, Leuven, Belgium, in 1986 and 1990, respectively. Since 2004, he is a Full Professor at the Electrical Engineering Department, Katholieke Universiteit Leuven, where he is currently heading a research team of 16 Ph.D. candidates and Postdocs, working in the area of signal processing for digital communications, wireless communications, DSL, and audio signal processing. He received the 1994 K. U. Leuven Research Council Award, the 1997 Alcatel Bell (Belgium) Award (with Piet Vandaele), and was a 1997 Laureate of the Belgium Royal Academy of Science. He was the Chairman of the IEEE Benelux Signal Processing Chapter (1998–2002), and is currently a EURASIP AdCom Member (European Association for Signal, Speech, and Image Processing, from 2000 till now). He is the Editor-in-Chief for the EURASIP Journal on Applied Signal Processing (from 2003 till now), and a Member of the Editorial Board of Integration, the VLSI Journal, IEEE Transactions on Circuits and Systems II (2002–2003), EURASIP Journal on Wireless Communications and Networking, and IEEE Signal Processing Magazine.